Selective hydroxylation of highly branched fatty acids and their derivatives by CYP102A1 from *Bacillus megaterium*

Michael Budde[a], Michael Morr[b], Rolf D. Schmid[a], Vlada B. Urlacher[a]

[a] *M. Budde, Prof. Dr. R. D. Schmid, Dr. V. B. Urlacher*

Institute for Technical Biochemistry, University of Stuttgart, Allmandring 31, 70569 Stuttgart, Germany

Fax: (+49) 711 685 3196

E-mail: itbvur@itb.uni-stuttgart.de

[b] *Dr. M. Morr*

Gesellschaft für Biotechnologische Forschung, Mascheroder Weg 1, 38124 Braunschweig, Germany

Fax: (+49) 531 6181795

E-mail: mmo@gbf.de

Abstract

Highly branched fatty acids, representing the main component of the preen gland wax of the domestic goose, and their derivatives are promising chiral precursors for the synthesis of macrolid antibiotics. The key step in utilisation of these compounds is the regioselective hydroxylation, which can not be done in a classical chemical approach.

Three P450 monooxygenases CYP102A1, CYP102A2 and CYP102A3, demonstrating high turnover numbers in hydroxylation of iso and anteiso fatty acids (>400 min^{-1}), were tested for their activity towards these substrates. CYP102A1 from *Bacillus megaterium* as well as its A74G F87V L188Q triple mutant hydroxylate a variety of these substrates with high activity and regioselectivity. In all cases the triple mutant showed much higher activities than the wild type enzyme. The binding constants, determined for CYP102A1 wild type and the triple mutant were >200 μM and ~23 μM, respectively, when tetramethyl nonanol was used as substrate. The data derived from binding analysis supports the differences in activity found for the CYP102A1 wild type and the triple mutant.

Surprisingly the CYP102A2 and CYP102A3 from *Bacillus subtilis* did not show activity at all. Substrate binding spectra, recorded to investigate substrate accessibility to the enzyme's active site, revealed that the substrates either could not access the active site of the *Bacillus subtilis* monooxygenases, or did not reach the heme proximity.

Keywords:

Branched chain fatty acids • Binding spectra • Polyketides • Cytochrome P450 • P450 BM-3 • monooxygenases

Introduction

Cytochrome P450s are ubiquitous, heme containing monooxygenases, which are able to introduce molecular oxygen at non-activated C-H-bonds.[1,2] The reduction equivalents, required for heme-iron reduction, are supplied by NAD(P)H and transferred via a flavoprotein and/or iron-sulphur proteins.[3]

The monooxygenases described in this paper, CYP102A1 from *Bacillus megaterium* (also referred to as P450 BM-3), CYP102A2 and CYP102A3 from *Bacillus subtilis* are fusion proteins consisting of a FAD/FMN containing reductase and a P450 monooxygenase in one polypeptide chain, thus exhibiting high turnover rates compared to other P450s. They are highly homologous regarding amino acid sequence (~60% identity for the overall enzyme; 63.8% (A1-A2) and 65.0% (A1-A3) for the monooxygenase domains). Earlier investigations on CYP102A1 showed that this monooxygenase is under control of the Bm3R1 repressor in *B. megaterium*. The repressor is inhibited by a wide range of compounds that are known to perturb lipid metabolism, e.g. barbiturates, hypolipidemic drugs and anti-inflammatory drugs. Polyunsaturated fatty acids which are toxic for *B. megaterium* are also potent inhibitors of Bm3R1 implying that CYP102A1 is probably responsible for fatty acid detoxification.[4] In contrast, CYP102A2 and CYP102A3 are not involved in an adaptive cell response leading to fatty acid detoxification.[5] Anyway, saturated as well as unsaturated fatty acids are hydroxylated by all three enzymes with high activities. Particularly interesting are iso and anteiso fatty acids, which are hydroxylated by CYP102A2 and CYP102A3 with turnover numbers being even one order of magnitude higher than those for non-branched saturated fatty acids.[6] These branched chain fatty acids (12-methylmyristic acid, 13-methylmyristic acid, 14-methylpentadecanoic acid and 15-methylpentadecanoic acid) play an essential role in membrane fluidity regulation in many bacteria (89% of all fatty acids in *B. megaterium* and 95% in *B. subtilis* are branched).[7]

Therefore CYP102A2 and CYP102A3 might be involved in regulation of the membrane fluidity by degradation of iso and anteiso fatty acids.

A logic consequence of these findings is the closer investigation of the reactivity of the cytochrome P450 monooxygenases towards branched chain fatty acids and their derivatives. Highly branched fatty acids, which can be found in the preen gland of the domestic goose or the muscovy duck are of particular interest, as they have polyketide-like structures with several chiral centres.[8] The regioselective functionalisation of such substances would offer a convenient route to new important pharmaceutical compounds like macrolide antibiotics. Many recent publications are dealing with post synthetic diversification of polyketides using, e.g. polyketide cytochrome P450 monooxygenases leading to structural diversity and biological activity of macrolides.[9,10]

So far classical chemical synthesis of macrolide antibiotics are complicated and contain e.g. iterative alkylation steps with a low overall yield. Enantioselective synthesis of the C1-C12 fragment of borrelidin, for example, requires 24 steps in total with an overall yield of 8%.[11] Regio- and enantioselective oxyfunctionalisation of available branched chain fatty acids is not possible by standard chemical methods and a separation of the produced regioisomers is unfavourable. Regioselective hydroxylation of e.g. 4,6,8-trimethyldecanoic acid with three defined chiral centres by a monooxygenase would provide a building block for the total synthesis of borrelidin. Other synthetic approaches using e.g. 2,4,6,8-tetramethyloctanol are also possible but require inversion of at least one chiral centre.

Here we describe the regioselective hydroxylation of highly branched fatty acids and derivatives by CYP102A1 wild type enzyme as well as its A74G F87V L188Q triple mutant. This mutant enzyme has been previously reported to have outstanding activity towards several different groups of chemical compounds, especially alkanes and alkanoic acids.[12] Additionally we

investigated binding behaviour of some of the tested compounds in the binding pocket of the P450 monooxygenases.

Materials and Methods

Chemicals

All chemicals were of analytical grade or higher quality and were purchased from Fluka (Buchs, Switzerland) or Sigma (Deisenhofen, Germany).

Enzyme expression and purification

Heterologous production of the enzymes in *E. coli* was done as described previously, using the pET28a+ expression system from Novagen (Madison, Wis., USA) for CYP102A1 and CYP102A2 wild types,[13] pET22 (Novagen) for the CYP102A3 wild type and the pCYTEXP1-vector for CYP102A1 A74G F87V L188Q.[14] All enzymes have been purified by anion exchange chromatography, using a Toyopearl DEAE-650M column from TosoHaas (Stuttgart, Germany). The enzymes were eluted with a linear gradient of NaCl (0 - 1 M) in potassium phosphate buffer (50 mM, pH 7.5).

Enzyme activity measurements

The P450 enzyme concentration was calculated from the corresponding CO difference spectra as described elsewhere using an extinction coefficient of 91 mM^{-1} cm^{-1}.[15] NADPH oxidation assay was used to measure enzyme activity towards different compounds. Therefore a 1 ml cuvette reaction setup was used, containing 50 mM potassium phosphate buffer pH 7.5, 0.1 µM enzyme solution, 2% (v/v) DMSO and 0.2 mM of substrate. The reaction was started by addition of 100 µl of aqueous NADPH solution (1.2 mM) and the cofactor consumption was tracked by absorption decrease at 340 nm with a photometer (Ultrospec 3000; Amersham Biosciences, Sweden). The slope within the first 20 seconds was used to determine initial activity. NADPH concentration decrease was calculated using an extinction coefficient of 6.22 mM^{-1} cm^{-1}.

Kinetic constants measurements

K_M, v_{max} and k_{cat} values were determined using a 1ml cuvette setup. The reaction mixture contained 50 mM potassium phosphate buffer pH 7.5, monooxygenase (0.1 µM for the triple mutant, 1.4 µM for wild type), DMSO (2%), substrate (0.01 to 0.4 µM). The reaction was started by addition of 100 µl of NADPH solution (1.2 mM). NADPH consumption was measured over 20 s to receive initial activity values. The data were fitted to a Michaelis-Menten kinetic.

Product analysis

After one hour of incubation to ensure the reaction completion, the reaction mixture (as described above) was extracted three times with diethyl ether and the combined organic phases were dried over anhydrous magnesium sulphate. The organic solvent was removed by a gentle stream of nitrogen and the residue was dissolved in 50 µl of N, O-bis(trimethylsilyl)trifluoroacetamide (BSTFA) + 1% (v/v) trimethylchlorosilane. The solution was transferred into a glass vial and incubated at 75°C for 20 min to yield trimethylsilylated products.

GC/MS analysis was carried out on a Shimadzu QP2010 instrument (column: FS-Supreme-5, length: 30 m, internal diameter: 0.25 mm, film thickness: 0.25 µm), using electron-impact ionisation (EI). The GC was temperature programmed as follows: injector: 250°C; oven: 100°C 1 min iso, 15°C min^{-1}, 300°C.

The products were identified using their characteristic mass fragmentation patterns. Product formation was calculated from GC peak area ratios and related to the amount of NADPH added, revealing coupling efficiencies.

Binding spectra

Substrate binding spectra were measured as described elsewhere using 500 µl of purified enzyme solution with an enzyme concentration of 5 to 10 µM.[16] A solution of substrate in DMSO was added subsequently to reach a final substrate concentration between 0.5 to 500 µM depending on substrate and enzyme. A reference sample containing enzyme solution and the appropriate amount of DMSO was used.

For determination of K_d, the reciprocal values of the absorption difference between 390 nm and 420 nm were plotted against the reciprocal values of the substrate concentration.

Results and Discussion

Hydroxylation of iso and anteiso fatty acids

CYP102A1, CYP102A2, CYP102A3 wild type and the triple mutant CYP102A1 A74G F87V L188Q were overexpressed in *E. coli* and purified by anion exchange chromatography as described in the materials and methods section. The purity of all three enzyme preparations reached that described previously for CYP102A1.[17] The SDS-PAGE is representative for the purification of all enzyme preparations used and shows the grade of purification for the CYP102A1 A74G F87V L188Q mutant (Figure 1).

The spectroscopic analysis revealed that all enzymes were actively expressed in *E. coli* (yield: appr. 400 mg l^{-1}). The purified enzyme preparations were used for activity screening towards branched chain fatty acids and their derivatives, based on the oxidation of NADPH. To avoid the detection of unspecific reactions during the NADPH oxidation assays, all reactions have been additionally performed with *E. coli* cell lysate as a negative control.

In the first experiment 13-methylmyristic acid and 12-methylmyristic acid (iso and anteiso pentadecanoic acid), which play an important role in membrane fluidity regulation of many

bacteria, were used as substrates for the wild type enzymes (Tables 1 and 2). Kinetic constants for CYP102A2 and CYP102A3 with these substrates were published recently,[5] however, not for CYP102A1. The coupling efficiencies, meaning the amount of NADPH actually used for product formation, were between 32% and 42% in general. Significant differences in initial activity of these monooxygenases were detected. Highest activity was measured for CYP102A2 towards 13-methylmyristic acid (2950 min^{-1}) and 12-methylmyristic acid (3600 min^{-1}), followed by CYP102A1 (1850 min^{-1} towards 13-methylmyristic and 1900 min^{-1} towards 12-methylmyristic acid). CYP102A3 shows comparably low activity (800 min^{-1} for 13-methylmyristic and 450 min^{-1} for 12-methylmyristic acid). The hydroxylation patterns were very similar for all three enzymes, represented by a mixture of ω to ω-6 hydroxylated products. The low regioselectivity in this hydroxylation is further evidence that these enzymes are involved in a first step in degradation of iso and anteiso fatty acids.

Screening with highly branched fatty acids and their derivatives

Encouraged by the high activities found, we screened a variety of branched chain fatty acids derived from the preen gland wax of the domestic goose and the muskovy duck (substrates **1** to **16**, Table 3). The investigated substance classes cover fatty acids, alcohols, methyl esters, ketones and one chlorinated compound with carbon chain lengths from eight to eleven and three to four branched methyl groups. A photometric NADPH oxidation assay as described above was used for preliminary substrate screening, and the formed products were identified using GC/MS analysis as described in materials and methods. The preliminary substrate screening was performed using identical reaction conditions with relatively low substrate (0.2 mM) and NADPH (0.4 mM) concentrations. Therefore, the data obtained allowed to compare activities between

different monooxygenases towards different substrates. Besides that, coupling efficiencies in all cases have also been calculated.

CYP102A1 wild type does show activity towards several of the tested substrates and product formation for substrates **2**, **3**, **4**, **5**, **7**, **8**, **9**, **10**, **12**, **14** and **16** was observed (Table 3). Educts with a carbon chain length between eight and eleven carbon atoms were hydroxylated at ω-1 position exclusively, if the ω-2 position is branched, and at ω-2 position, if the ω-2 position is not branched. The high regioselectivity of CYP102A1 in these reactions is particularly remarkable, as CYP102A1 and its mutants usually oxidize saturated fatty acids at subterminal (ω-1, ω-2, ω-3) positions, producing a mixture of differently hydroxylated products.[18,19]

Alcohols were accepted as substrates rather than the corresponding acids, which is in contrast to the results found for non-branched fatty acids and alcohols.[20] Generally the activities of wild type CYP102A1 towards all accepted substrates was quite low (~ 10 – 40 min^{-1}) as well as coupling efficiencies (10 – 50 %).

A recently described triple mutant (CYP102A1 A74G, F87V, L188Q) showing outstanding activity towards alkanes and many other substances was also investigated.[12] This mutant indeed turned out to be more active towards the compounds tested, exhibiting initial turnover rates between 118 eq min^{-1} and 1218 eq min^{-1} as well as high coupling efficiencies (e.g. >80% for substrates **3**, **9**, **10**). All substrates apart from **1** (a fatty acid with the shortest carbon chain (C8) among the substrates tested) and **15** (a substrate containing a cyclopropyl unit) were hydroxylated by the triple mutant. Also here, most substrates were hydroxylated with exceptional regioselectivity: those beeing branched at ω-2 position were hydroxylated at ω-1 exclusively; however the regioselectivity of the enzyme in reactions with substrates **11**, **12**, **13** and **14,** having unbranched ω-1 and ω-2 positions was low. In the latter case the ω-1 and ω-2 positions were hydroxylated and no preference for ω-1 or for ω-2 was observed. For a selective hydroxylation of

substrates **12** and **14** at ω-2 position, CYP102A1 wild type could be used (ω-2 >94% regioselectivity).

As substrate **6, 10** and **16** were of special interest as suitable building blocks in synthesis of borrelidin, their catalytic constants were calculated (Table 4). Compared to the experiments for estimation of coupling efficiency, higher concentrations of corresponding substrates were used. In all cases kinetic data were fitted to Michaelis-Menten kinetics. The compound 6 was identified as the best substrate for the triple mutant (k_{cat}=1512 min^{-1}, K_M=670 μM), although the wild type did not produce any products in this reaction. The initial activity determined in the preliminary screening is lower than the measured k_{cat}-value as the substrate concentration used in the screening (0.2 mM) was significantly below the K_M-value. Compounds **10** and **16** are also accepted by CYP102A1 as substrates, but converted only with little activity (k_{cat}= 59.5 min^{-1}, K_M= 530 μM for **10**; k_{cat}=150.7 min^{-1}, K_M=47 mM for **16**) compared to the triple mutant (k_{cat}= 666.7 min^{-1}, K_M= 67 μM for **10**; k_{cat}=939.9 min^{-1}, K_M=150 μM for **16**).

The products derived from these reactions can directly be used in borrelidin synthesis. The very complex separation of several hydroxylated products can be avoided.

The CYP102A2 and CYP102A3 wild types showed no NADPH consumption at all with the tested substances. After several hours of incubation at room temperature no product could be detected by GC/MS in the reaction extracts, although iso- and anteiso fatty were converted with high turnover numbers between 450 and 3600 per minute.

To further examine this circumstance, we recorded substrate binding spectra to check, whether the substrates can reach the active site and if they show e.g. an inhibitor type binding spectrum.

Binding spectra

Substrates **6** and **10** have been chosen for enzyme characterisation. A characteristic type I binding spectrum was obtained during the titration of CYP102A1 A74G F87V L188Q with substrate **6** leading to a shift in the spin-state equilibrium of the heme-iron towards the high-spin form (Figure 2). This is indicated by an absorption increase at 390 nm and a decrease at 422 nm. Titration with substrate **10** also induced a type I spectrum. The absorption differences between 390 nm and 420 nm were plotted versus the corresponding substrate concentrations revealing a hyperbolic curve progression. The K_d-values for the triple mutant have been determined to K_d = 26.2 μM with **10** and K_d = 23.2 μM with **6**. This implies an optimal positioning of the substrates at the active site with simultaneous replacement of water and their high affinity to the enzyme.[21] Titrations of CYP102A1 wild type with both substrates lead to an absorption increase at 420 nm and a decrease at 390 nm, resulting in reverse type I binding spectra (Figure 3). Here much higher substrate concentrations (up to 475 μM) were required to perturb the spin state equilibrium. The absorption differences ascend linearly with increasing substrate concentrations. Saturation concentrations could not be reached due to the low solubility of the substrate, but K_d certainly was higher than 200 μM. Observation of reverse type I spectra is frequently accounted to a non-displaced water molecule as sixth ligand of the heme iron, being evidence for poor substrate binding.[22] This is in accordance with the low overall activity of the wild type towards the substrates tested. Obviously the exchange of three amino acids (F87, A74 and L188) has a high influence on correct positioning of the substrates. Phenylalanine 87 is located over the heme active site and substitution by alanine increases the size of the binding pocket. Exchange of alanine 74 to glycine increases local flexibility and reduces steric interactions with the substrate within the access channel. Position 188 also is a part of the substrate access channel and already proved to have impact on carboxylate binding when lysine or glutamine are introduced.[23]

Titration of CYP102A2 and CYP102A3 with both substrates was carried out analogously, but even with high substrate concentrations (> 500 μM) no spin state perturbation was observed, indicating that the substrates do not bind in the binding pocket or do not reach the heme group.

If one considers the high identity among CYP102A1, CYP102A2 and CYP102A3 including identity of crucial amino acids close to the heme active site, e.g. F87/88, L437/439, L181/182, I263/265, A264/266, the differences found in the substrate spectra are remarkable (Figure 4). The residues located in the middle of the access channel (positions 72, 74, 75 in A1, 73, 75, 76 in A2 and A3) are also similar. The major difference here is the position 72/73, where A1 contains a serine, A2 a glutamate and A3 a glycine. The most obvious differences in amino acid sequence can be found at the entrance of the substrate access channel (positions 42/43, 47/48, 51/52), where CYP102A3 and especially CYP102A2 have smaller amino acids. One would therefore expect that sterically more demanding substrates will reach the active centre of CYP102A2 and A3 more easily compared to CYP102A1. However as shown by the substrate binding spectra, the branched chain substrates do not reach the heme group. One explanation might be that in case of CYP102A2 arginine 354 blocks the access channel. CYP102A1 has an arginine 47 located at the entrance of the access channel, which is involved in fatty acid binding. In CYP102A3 glycine 73 might change the active site structure such, that bulkier substrates are also hindered from entering the active site. This is an issue which is not addressed by a simple homology model based on the CYP102A1 crystal structure.[24] A crystal structure of the two *Bacillus* CYP's might help to understand the differences in substrate accessibility.

The selective hydroxylation of highly branched fatty acids and derivatives provides an easy access to chiral precursors for the production of polyketides. The use of cytochrome P450 monooxygenases, especially the CYP102A1 A74G F87V L188Q triple mutant, for regioselective hydroxylation of substrates derived from the preen gland wax of the domestic goose opens an

easy route towards macrolidic compounds, which are of high pharmaceutical value. Multistep chemical reactions with low total yield and sophisticated purification procedures can be avoided.

References

[1] D. Werck-Reichhart, R. Feyereisen, *Genome Biol.* **2000**, *1*, REVIEWS 3003.

[2] L. L. Wong, *Curr. Opin. Chem. Biol.* **1998**, *2*, 263.

[3] K. J. McLean, M. Sabri, K. R. Marshall, R. J. Lawson, D. G. Lewis, D. Clift, P. R. Balding, A. J. Dunford, A. J. Warman, J. P. McVey, A. M. Quinn, M. J. Sutcliffe, N. S. Scrutton, A. W. Munro, *Biochem. Soc. Trans.* **2005**, *33*, 796.

[4] C. N. A. Palmer, E. Axen, V. Hughes, C. R. Wolf, *J. Biol. Chem.* **1998**, *273*, 18109.

[5] M. C. Gustafsson, C. N. Palmer, C. R. Wolf, C. von Wachenfeldt, *Arch. Microbiol.* **2001**, *176*, 459.

[6] M. C. Gustafsson, O. Roitel, K. R. Marshall, M. A. Noble, S. K. Chapman, A. Pessegueiro, A. J. Fulco, M. R. Cheesman, C. von Wachenfeldt, A. W. Munro, *Biochemistry* **2004**, *43*, 5474.

[7] T. Kaneda, *Microbiol. Rev.* **1991**, *55*, 288.

[8] M. Morr, V. Wray, J. Fortkamp, R. D. Schmid, *Liebigs Ann. Chem.* **1992**, 433.

[9] Y. J. Yoon, B. J. Beck, B. S. Kim, H. Y. Kang, K. A. Reynolds, D. H. Sherman, *Chem. Biol.* **2002**, *9*, 203.

[10] Y. Q. Xue, D. Wilson, L. S. Zhao, H. W. Liu, D. H. Sherman, *Chem. Biol.***1998**, *5*, 661.

[11] B. G. Vong, S. Abraham, A. X. Xiang, E. A. Theodorakis, *Org. Lett.* **2003**, *5*, 1617.

[12] D. Appel, S. Lutz-Wahl, P. Fischer, U. Schwaneberg, R. D. Schmid, *J. Biotechnol.* **2001**, *88*, 167.

[13] M. Budde, S. C. Maurer, R. D. Schmid, V. B. Urlacher, *Appl. Microbiol. Biotechnol.* **2004**, *66*, 180.

[14] Q.-S. Li, U. Schwaneberg, P. Fischer, R. D. Schmid, *Chem. Eur. J.* **2000**, *6*, 1481.

[15] T. Omura, R. J. Sato, *J. Biol. Chem.* **1964**, *239*, 2370.

[16] M. A. Noble, C. S. Miles, S. K. Chapman, D. A. Lysek, A. C. MacKay, G. A. Reid, R. P. Hanzlik, A. W. Munro, *Biochem. J.* **1999**, *339*, 371.

[17] U. Schwaneberg, A. Sprauer, C. Schmidt-Dannert, R. D. Schmid, *J. Chromatogr. A* **1999**, *848*, 149.

[18] G. Truan, M. R. Komandla, J. R. Falck, J. A. Peterson, *Arch Biochem Biophys* **1999**, *366*, 192.

[19] A. Glieder, E. T. Farinas, F. H. Arnold, *Nat Biotechnol* **2002**, *20*, 1135.

[20] Y. Miura, A. J. Fulco, *Biochim. Biophys. Acta* **1975**, *388*, 305.

[21] S. A. Maves, H. Yeom, M.cLean, S. G. Sligar, *FEBBS lett.* **1997**, *414*, 213

[22] J. B. Schenkman, S. G. Sligar, D. L. Cinti, *Pharmacol. Ther.* **1981**, *12*, 43.

[23] Q.-S. Li, U. Schwaneberg, M. Fischer, J. Schmitt, J. Pleiss, S. Lutz-Wahl, R. D. Schmid, *Biochim. Biophys. Acta* **2001**, *1545*, 114

[24] H. Li, T. L. Poulos, *Nat Struct Biol* **1997**, *4*, 140.

Figure legends:

Figure 1.

SDS-PAGE analysis of purification of CYP102A1 A74G F87V L188Q by anion exchange chromatography on a DEAE 650 column. Lane 1: cell lysate: lane 2: column flow-through; lane 3: purified fraction; M: molecular weight standard.

Figure 2.

Type I binding spectra resulting from the titration of CYP102A1 A74G F87V L188Q with **6**. Absorbance increases at 390 nm and decreases at 420 nm with increasing substrate concentrations. Inset: Absorption difference between 390 nm and 420 nm plotted against the substrate concentration.

Figure 3.

Reverse type I binding spectra resulting from the titration of CYP102A1 wild type with **6**. Absorbance decreases at 390 nm and increases at 420 nm with increasing substrate concentrations. Inset: Absorption difference between 420 nm and 390 nm plotted against the substrate concentration.

Figure 4.

Crystal structure of CYP102A1 (**A**) and homology models of CYP102A2 (**B**) and CYP102A3 (**C**). The active sites and the substrate access channels are shown including palmitic acid as substrate and the heme group (both displayed in black).

Tables

Table 1.

Hydroxylation of 13-methylmyristic acid

Enzyme CYP102	NADPH consumption [min^{-1}]	Coupling efficiency [%] [%]	Regioselectivity					
			ω-1	ω-2	ω-3	ω-4	ω-5	ω-6
A1	1850	32	1	18	76	5	-	-
A2	2950	38	-	7	91	2	-	-
A3	800	35	-	6	89	5	-	-

Table 2.

Hydroxylation of 12-methylmyristic acid

Enzyme CYP102	NADPH consumption [min^{-1}]	Coupling efficiency [%] [%]	Regioselectivity					
			ω-1	ω-2	ω-3	ω-4	ω-5	ω-6
A1	1900	38	1	57	12	20	1	9
A2	3600	42	1	53	16	19	-	11
A3	450	32	1	27	16	36	4	16

Table 3.

Hydroxylation of branched chain hydrocarbons by CYP102A1 wild type (WT) and the A74G F87V L188Q triple mutant (3xMut). Tetramethyl-branched hydrocarbons are derived from the preen gland wax of the domestic goose; trimethyl-branched hydrocarbons are from the muscovy duck. Initial activity is given in nmol of NADPH per nmol of enzyme per minute.

Substrate No.	Structure	NADPH-consumption [min^{-1}]		Regioselectivity ω-1: ω-2		Coupling efficiency [%]	
		WT	3xMut	WT	3xMut	WT	3xMut
1	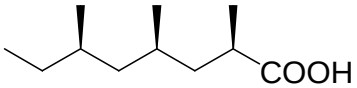	2	31	n.d.	n.d.	n.d.	n.d.
2	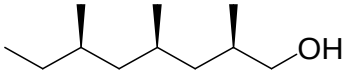	37	1204	100:0	100:0	35	50
3	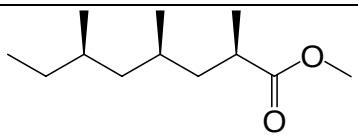	11	1218	100:0	100:0	21	>90
4	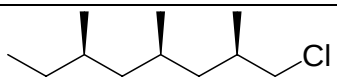	13	312	100:0	100:0	50	62
5	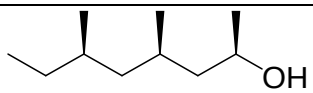	18	759	100:0	100:0	3	28
6	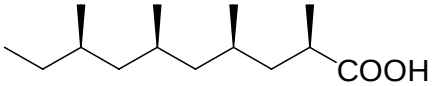	18	507	n.d.	100:0	n.d.	22
7	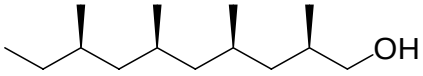	28	595	100:0	100:0	28	73

8	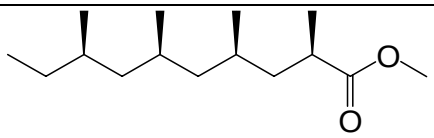	15	265	100:0	100:0	7	43
9	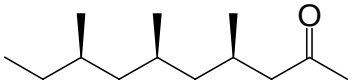	16	707	100:0	100:0	72	83
10	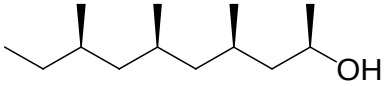	38	765	100:0	100:0	45	83
11	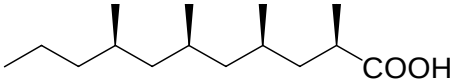	28	720	n.d.	67:33	n.d.	35
12	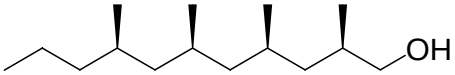	33	373	6:94	29:71	30	40
13	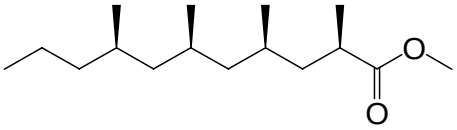	16	119	n.d.	45:55	2	17
14	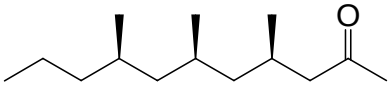	41	562	4:96	64:36	40	42
15	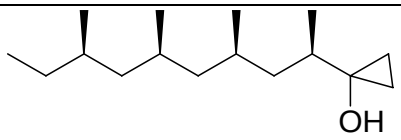	21	15	n.d.	n.d.	n.d.	n.d.
16	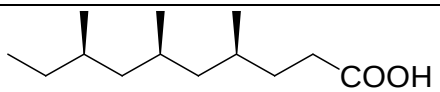	51	590	100:0	100:0	8	23

Table 4.

Catalytic constants for CYP102A1 wild type and the triple mutant with three different substrates.

		A1 wild type			Triple mutant	
Substrate No.	K_M [mM]	v_{max} [mM min^{-1}]	k_{cat} [min^{-1}]	K_M [μM]	v_{max} [mM min^{-1}]	k_{cat} [min^{-1}]
6	-	-	-	670	0.23	1512
10	0.53	0.08	59.5	35.08	0.07	666.7
16	47	0.02	150.7	150	0.09	939.9

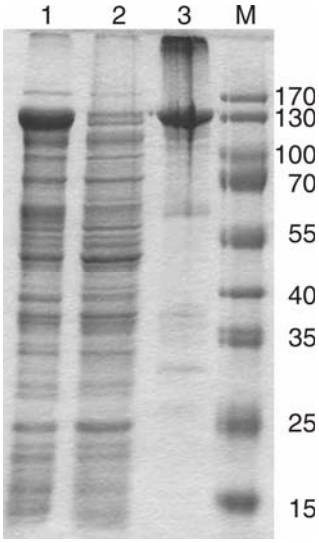

Figure 1.

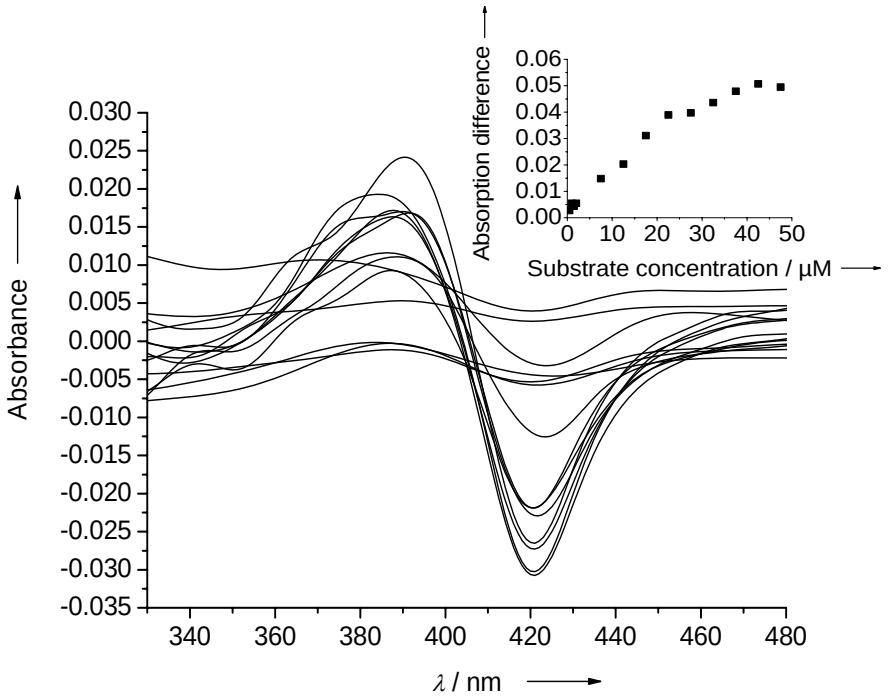
Absorbance
0.030
0.025
0.020
0.015
0.010
0.005
0.000
-0.005
-0.010
-0.015
-0.020
-0.025
-0.030
-0.035
340
360
380
400
420
440
460
480
λ / nm
Absorption difference
0.06
0.05
0.04
0.03
0.02
0.01
0.00
0
10
20
30
40
50
Substrate concentration / µM

Figure 2.

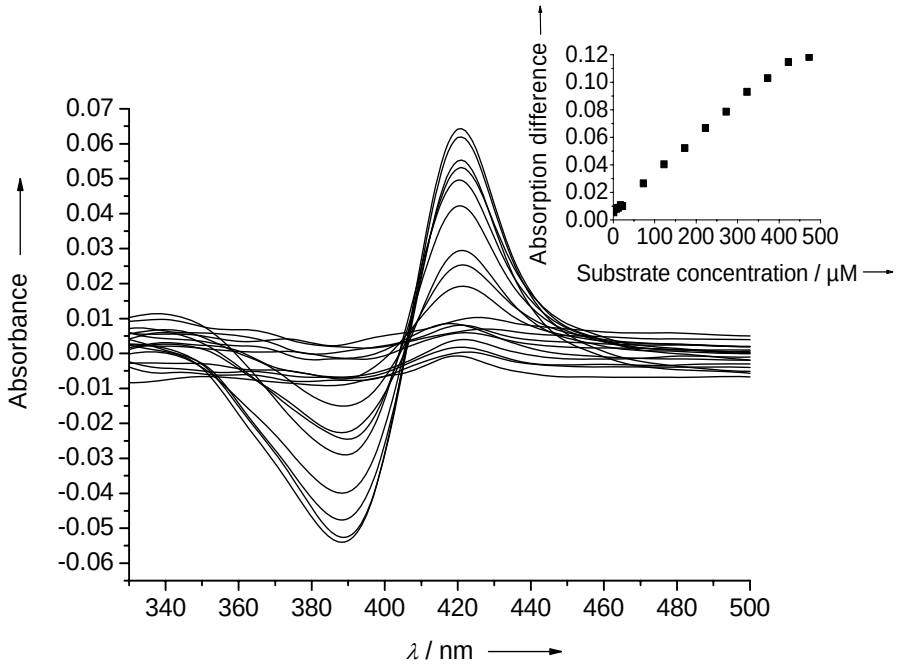
Absorbance
0.07
0.06
0.05
0.04
0.03
0.02
0.01
0.00
-0.01
-0.02
-0.03
-0.04
-0.05
-0.06
340
360
380
400
420
440
460
480
500
λ / nm
Absorption difference
0.12
0.10
0.08
0.06
0.04
0.02
0.00
0
100
200
300
400
500
Substrate concentration / µM

Figure 3.

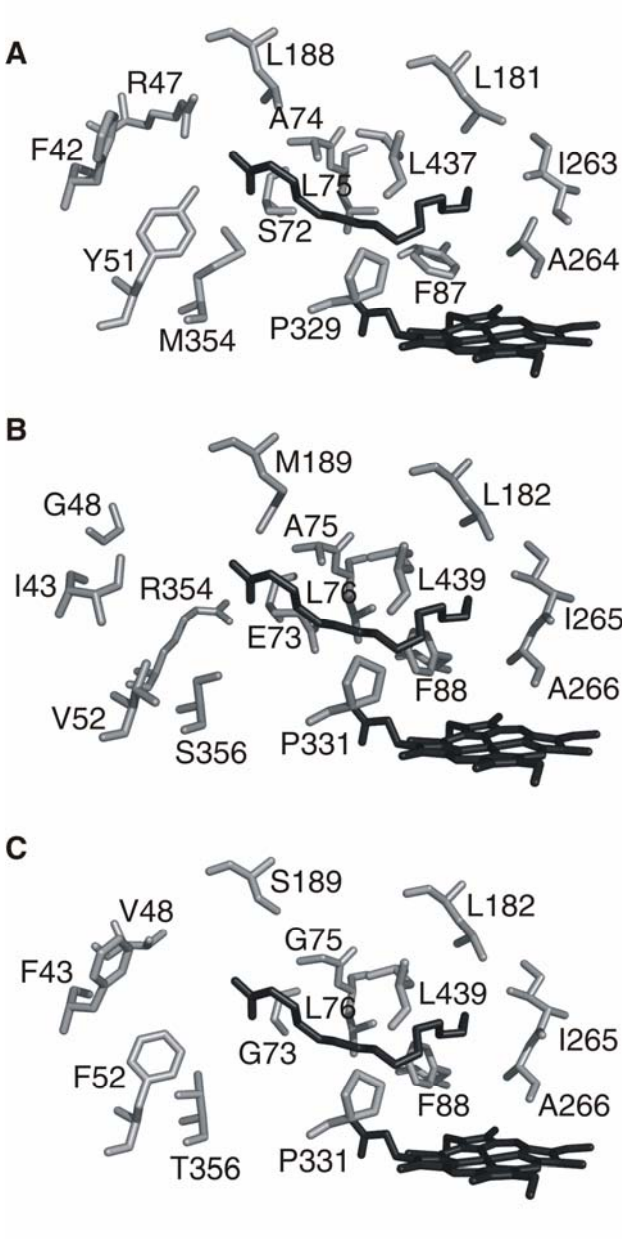
A
L188
R47
L181
A74
F42
L437
I263
L75
S72
Y51
A264
F87
M354
P329
B
M189
L182
G48
A75
I43
R354
L76
L439
I265
E73
F88
A266
V52
S356
P331
C
S189
L182
V48
G75
F43
L76
L439
I265
G73
F52
F88
A266
T356
P331

Figure 4.